# Quality Excellence in *Battery Cell* Production:

## The Power of Process Simulation

in partnership with

Capgemini

Fraunhofer FFB | PEM | RWTH AACHEN UNIVERSITY | PEM MOTION

# Content

# Management Summary

This study demonstrates that process simulation is a strategic tool for enhancing battery cell production, as exemplary demonstrated on the electrode drying process. By providing a deeper understanding of production processes and enabling precise adjustments, it offers significant economic and technological benefits. Manufacturers adopting this approach can expect reduced scrap rates, estimated **up to 3% in long term scrap reduction**, if fully implemented, thus saving up to **138 Mio. €** per year for 50 GWh of cell production.

The benefits include:

1. **Enhanced Understanding of Production Processes:**
   Process simulation provides a detailed understanding of the physical processes involved in battery cell production, allowing manufacturers to optimize parameters and improve product quality.
2. **Scalability and Transferability:**
   The process models developed can be applied across multiple production lines and sites, making them highly scalable and cost-efficient.
3. **Improved Equipment Utilization:**
   Simulation models help in understanding the interplay between equipment and product, enabling better utilization of machinery and reducing trial-and-error adjustments.
4. **Accelerated Development and Industrialization:**
   The use of simulation can cut development time by up to 50%, facilitating faster transitions from pilot to giga-scale production and ensuring timely delivery of high-quality battery cells.
5. **Sustainable Long-Term Benefits:**
   Process simulation raises the level of understanding of individual processes, leading to continuous improvements and sustainable benefits for manufacturers.

> **The product quality and consequently the profitability of battery cell production is determined by the level of understanding of your production process.**
> **The player with the most accurate physics-based simulation models of its production processes will likely lead the market.”**
>
> **Michael Müller, Head of Climate Tech & Sustainability, Capgemini**

# 01. Introduction

The European battery industry has left the start-up phase and in recent years entered into the scale up and mass production phase, which has shown to be highly challenging [1]. Among others, problems such as quality in cell production and high scrap rates were cited as well as a lack of talent. Without qualified and experienced personnel, the manufacturers are required to build and retain the necessary production know-how and a deep understanding of the interplay between machinery and product, which are key for the success of battery cell production. While machinery can be purchased easily on the market, mostly from Asian suppliers, the specific understanding of the machine adjustments and fine tuning of parameters to meet the high-quality standards demanded for Li-ion battery cells is often missing and needs to be built over years. Additionally, these skills are not always fully transferable as the problems arising during production can be quite specific to the individual cell design.

The first steps in cell production, from mixing to calendaring, have been identified as crucial and can be a source for high scrap rates or low cell performance. Problems such as high variation in slurry output viscosity after mixing or carbon-binder migration from rapid drying in high loading electrodes can arise. Better understanding of these processes and the influence of the machinery on electrode quality is needed to address such issues and help manufacturers understand their equipment and product.

Here, we would like to introduce our approach to support cell manufacturers in gaining a better understanding of the ongoing processes by virtue of process simulation.

**Our objective is to involve process engineers and tackle their challenges, to deliver lasting process improvements.**

The general principle behind process simulation is to re-create the physical process during cell production, for example when physical processes such as flow of liquids (e.g., slurry during coating or electrolyte during filling) or solvent evaporation (i.e., drying of coatings) occur. The models are not limited to the presented electrode production steps, other models representing processes such as electrode drying or cell filling, are also viable. Such models become industrially relevant when the model contains not just a 1D or 2D cutout of the process, but the process in its entirety, including the machinery and relevant surroundings.

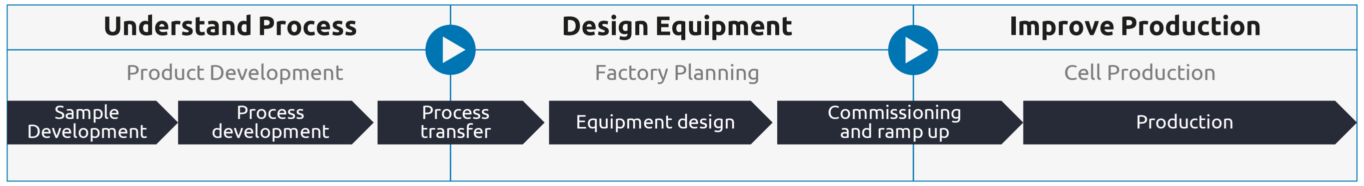

Figure 1: Overview of the main benefit across the battery cell production stages.

Industrially relevant modelling should link the model to the machinery input as well as the product information, such that process engineers can directly transfer the model settings to their machinery. The model shows what would otherwise be a black-box process, giving an understanding of the impact of process parameter or design changes on the product quality.

Impact of such models can be found on various stages during development, factory planning and production, as shown in Fig. 1. During cell development, also the production processes are developed and adjusted to the new cell design. Especially during the material screening phase, process parameters may vary significantly and need to be adjusted regularly. Process models can support in parameter prediction and understanding the effect of product changes on the process. This understanding of the newly designed process is highly useful during the factory planning stage, where the scaled-up equipment can be adjusted to the developed requirements and tested virtually using the processing parameters required for large scale production. Thus, initial parameters for the ramp-up phase can be found, and process simulation can support in fine tuning the equipment for long term scrap reduction adjustments.

**For such a model we offer an all-in-one approach, where the necessary parametrization, model creation and validation are developed and performed within our network.**

In this publication, we first show a summary of our approach for the first four process steps, mixing, coating, drying and calendaring. To give a more in-depth understanding of the topic, we have chosen to demonstrate our combined approach for the process of electrode drying. We discuss the types of electrode drying models available in literature to give the interested reader an introduction to this specific topic. We then give a description of our modelling approach and subsequently demonstrate the parametrization of the drying process. The combination of model and experiment is used to fine tune the model to the specific properties of the slurry and its behavior during electrode drying. Lastly, we give an outlook on how the validation of the model can look like, by showcasing electrode drying on a roll-to-roll system with subsequent electrode analysis.

# 02. End-to-end toolchain from Mixing to Calendaring

In broad terms, an end-to-end (E2E) modelling toolchain contains processing models of all steps in the battery cell production process, with interconnected models and ending in a model of the final cell itself (e.g., a p2D Newman-type model). For example, during the coating process the slurry flow through the coating head and onto the substrate foil can be modelled through computational fluid dynamics (CFD) simulations, giving useful information on the effects of the coater design on the electrode homogeneity or edge quality.

**Process models can run in parallel during cell production and thus reduce testing efforts during production ramp up.**

But in practice, not all steps are useful to be modelled. The slitting or stacking process for example lack both an influence on parameters for electrode quality as well as a physical process to be modeled (please note that electrode quality is viewed from an electrode performance or cell model perspective, there are electrode quality parameters such as e.g., burr size, important for the overall cell quality, which are not relevant here). Similarly, sensibly interconnecting all models would be a major undertaking and is, as of yet, not part of our whitepaper. As mentioned above, after calendaring, electrode quality markers such as pore resistance (influenced by porosity and tortuosity), electrical resistance, adhesion or particle breaking are mostly settled. As such, in the long run the proposed models are ideally improved to reflect on these electrode properties, truly allowing to predict internal resistances.

Thus, as a first version of our E2E toolchain we describe in more detail models for the first four processing steps, mixing, coating, drying and calendaring. Other processes such as electrode roll drying, cell baking, electrolyte injection, cell degassing or gas generation during cell formation are also options to extend the E2E toolchain to further process steps.

### Overall model objectives:

The models described here are designed to support the process engineers in a cell manufacturing plant and provide a better understanding of the inner workings of the equipment or processes. They should additionally directly provide processing parameters or help the process engineer in finding those. Figure 2 shows an overview of this approach. As mentioned above, linking these models directly to electrode or cell performance parameters is, for this first approach, outside of the scope of these models, as these phenomena are not directly captured due to the high resource demand this would require. However, indirectly the electrode quality should be improved through the use of process simulation, as these models aim at improving the production processes itself. For example, improved electrode drying should also counteract carbon/binder migration, in turn reducing the electrodes internal resistance and improve adhesion. Thus, we believe that the process-centric approach is highly useful in improving electrode quality by directly supporting the production process.

**Process Modelling - Model of the physical process and equipment**

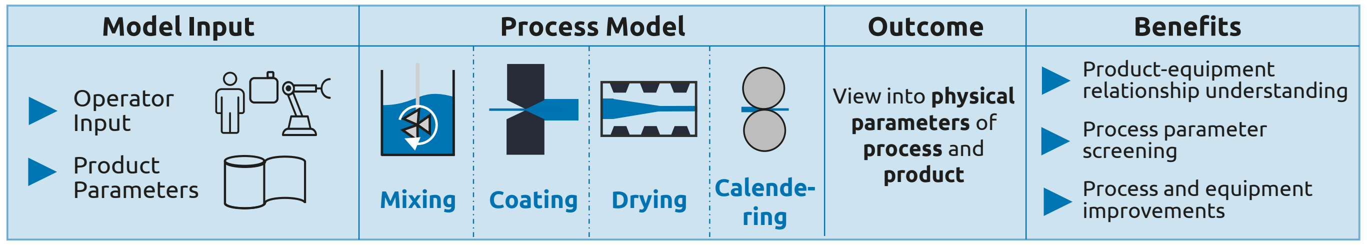

Figure 2: Process modelling overview

### Battery slurry mixing model description:

The battery slurry mixing step is among the most influential of the battery production steps when it comes to electrode quality. The required proper dispersion of active and passive materials during batch production requires a good understanding of the slurry behavior or the behavior of the added materials. This is especially crucial during A-sample development, where multiple materials are tested and need to be crafted into high quality electrodes in a short amount of time. The difficulties of the slurry mixing process lie in the influences of macroscopic as well as microscopic factors. Macroscopic factors that influence the slurry quality are e.g., the mixer design itself, the level of larger agglomerates in the raw powders that need to be broken or the speed and order in which the slurry is mixed. Simultaneously, microscopic factors can change the behavior of a slurry just as well, e.g. the binder chain length (represented by the molecular weight of the binder), the material quality parameters (e.g., remaining LiOH or Li2CO3 especially in combination with Ni-rich NMCs and PVDF binders) or factors such as over-mixing, which can lead to damages of the materials. Incorporating all these processes into a physical model would require the modelling of the entire mixing apparatus down to the molecular level, which is computationally not feasible.

Only for this process step, instead of building a physical model our approach is to use machine learning (ML) to truly cover the breadth necessary for the mixing process step. The ML model needs to be trained to the specific purpose:

(i) during Cell development, the production parameters of the slurry are changing quite often, thus a model trained on continuously changing material and processing input eventually gains an understanding of the complex interdependencies and can help predict processing input requirements for testing of new materials such as binders or active materials;

(ii) during cell production, input parameters and process should remain constant, thus the model would be trained for anomaly detection to find deviations during production. The aim is to reduce the spread in output quality by understanding the sources of such deviations

Important for machine learning models is the data quality, as such data cannot simply be dumped into a model, but requires careful screening from both a specialist of the mixing process itself as well as the data scientists responsible for building the model. If successfully implemented, such a model can help give the process engineer guidelines on the influence of material or process parameters on the process outcome, i.e., replacing what is otherwise intuition or long standing learning by professionals. The model would learn with every production run and thus build and retain knowledge for the cell manufacturer.

## Slurry coating model description:

After mixing, the ideally gas and agglomerate free slurry is transported to the coating step. It is therefore pumped into the coating head, from where it is pressed through a thin slit and onto the moving substrate foil. The slid width is usually manually adjusted in a set of bolts tightened at various intervals along the coating head. A metal plate, the shim plate, is specifically designed to achieve a desired coating thickness and to control the quality on the coating edge. Thus, the coater geometry and slurry rheology are important for coating homogeneity, proper mass loading and edge quality. Such a process can be recreated using CFD simulations, where the slurry is reduced to a homogeneous liquid with rheological properties determined from the incoming slurry. Such a model requires the detailed representation of the slurry coating head and substrate foil and operates under the assumption that the slurry is free of agglomerates or trapped gas bubbles. The information that can be gained from such a model is for example how the slurry rheological properties in combination with the coater shim plate result in a certain coating edge quality. Alternatively, the effect of changing rheological properties on the coating quality can be explored. For every production step, tolerances are defined for rheological properties, usually defined as a range in viscosity at a defined shear rate. Understanding the equipment’s behavior across the tolerance range can support the process engineer in defining the tolerances or understand how to adjust the equipment accordingly.

## Electrode drying model description:

The electrode drying step is shown in this whitepaper as an in-depth example, where we showcase how we model, parametrize and validate the process model. The underlying processes as well as our model approach is described in more detail in the following section 3.

## Calendaring model description:

During the calendaring step, the dried electrode is compressed to a previously defined thickness, a step that can improve electrode resistances (especially for cathodes) as well as electrode adhesion. Drawbacks can be particle cracking, which is especially impactful on poly-crystalline NMCs cycle life but should be avoidable by determining the proper calendaring thickness during the development stage. Furthermore, electrode processing can cause wrinkles in the bare foil edge, which needs to stay wrinkle free for later use as electrical contact to the cells current collector, which can be a major problem during later welding stages. This wrinkle formation is one sub-process where we see relevance in process modelling and propose modelling tension differences between the bare foil edge and the coated foil and coating while it is compressed. This gives insight into the root causes of foil wrinkling and allows virtual testing of different conditions, such as calendaring at various temperatures or local temperature induction, to find pathways to counteract this effect.

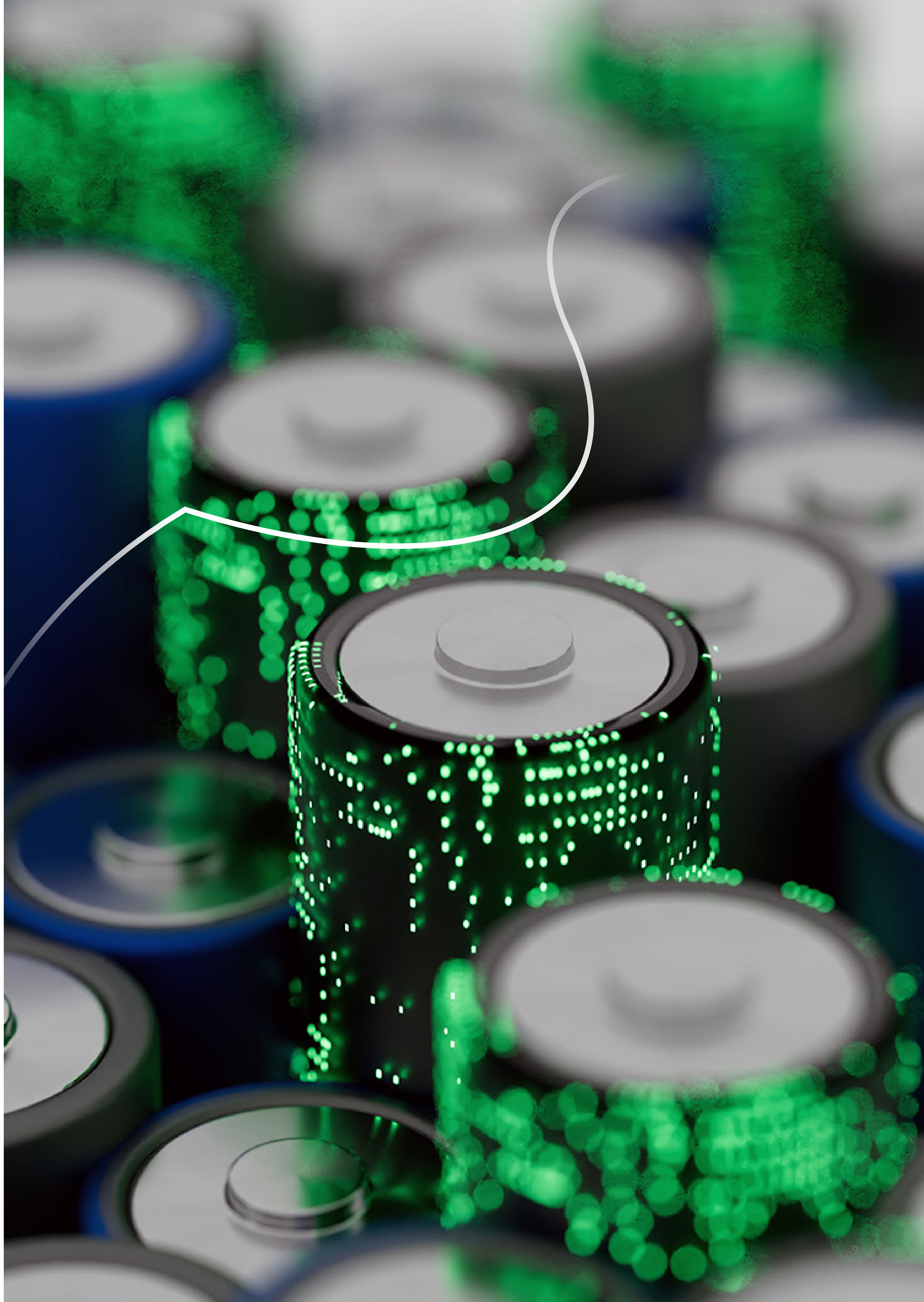

# 03. Electrode drying and approaches to modelling

In the following we outline the process step of electrode drying and give approaches on how to model it from existing literature.

## 3.1 Fundamentals of the electrode drying process

Convection drying is a widely used process in the production of battery electrodes and currently the state-of-the-art technology for electrode drying. After the application of the electrode suspension on the current collector in the coating process, the current collector with the wet film is introduced in the drying chamber. Heated air is then blown onto the coating through nozzles, introducing heat from above and below to evaporate the solvent and solidify the electrode layer. This method relies on the transfer of heat from the air to the wet film, causing the solvent to evaporate progressively. The drying rate and efficiency are influenced by parameters such as mass loading, solids content, and the thickness of the coating. Conventional convective drying typically achieves web speeds of 25 - 80 m/min, with potential future speeds of up to 100 m/min. However, increasing the drying rate can lead to segregation of binder and carbon black particles, negatively impacting the electrode's adhesive strength and overall quality. To mitigate these issues, a combination of convective and other drying technologies, such as infrared or laser drying, is often employed to enhance drying efficiency and reduce dryer length, thereby optimizing the production process.[2] The key components of the coating and drying process are depicted in Figure 3.

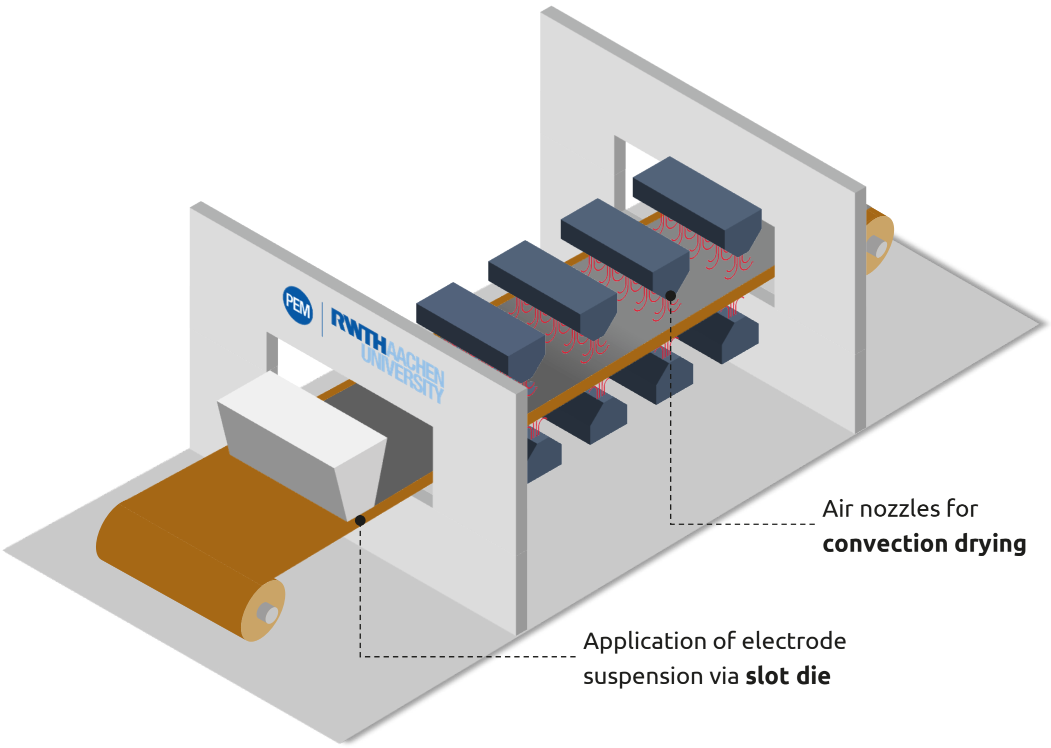

Figure 3: Sketch of the coating and convection drying of a battery electrode.

The electrode drying process involves five stages (Figure 3). Initially, a homogeneous wet film is formed where the slurry is evenly distributed across the current collector. As the solvent begins to evaporate, the film transitions into a consolidated wet film, where the particles start to coalesce and form a semi-solid structure. This stage is characterized by the initial aggregation of particles and the formation of a surface layer. Further evaporation leads to the formation of a partially filled capillary network, where the solvent is primarily located within the capillaries between the particles, causing the film to shrink and small particles to be carried to the surface. This stage is followed by isolated liquid pores, where the remaining solvent is confined to isolated pockets within the film, and the capillary forces continue to drive the solvent out. Finally, the process concludes with a consolidated dry film, where all the solvent has evaporated, leaving behind a solid, cohesive electrode coating with a well-defined porous structure. [3]

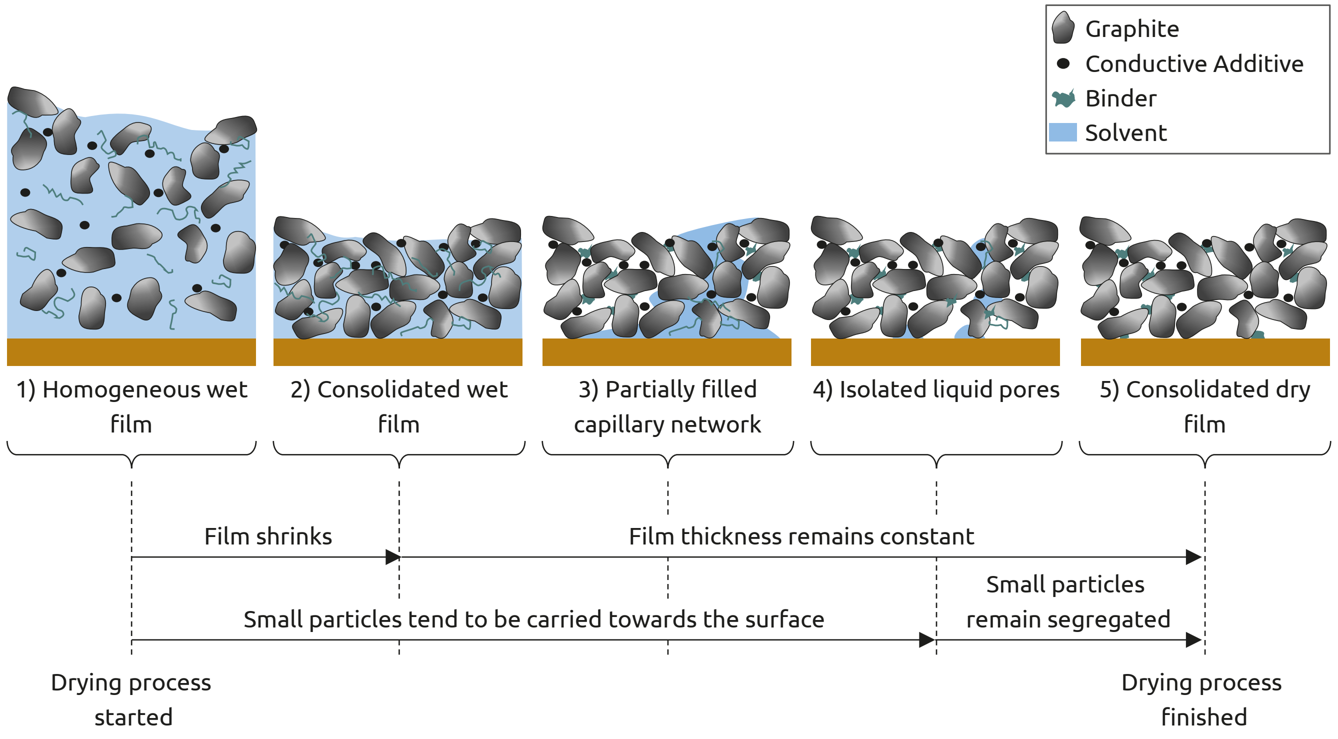

Figure 4: Stages of the electrode drying process (based on Kumberg et al. [4]).

## 3.2 Modelling approaches for the drying process in literature

There are different approaches to model the electrode drying process. Kumberg et al. [4] present a comprehensive study on the drying process of lithium-ion battery electrodes with varying thicknesses, combining experimental validation with simulation. The authors initially employ a linear drying kinetics model, which assumes no internal transport resistance, to predict solvent loading and film temperature. However, to address the limitations observed in thicker films, the model is extended to incorporate a moving drying front, accounting for transport resistances within the porous electrode structure. The simulation results, validated against an experimental setup with high precision scale, demonstrate that the extended model accurately captures the drying behavior of thicker electrodes, where capillary transport and film resistance significantly influence the drying kinetics. This study highlights the necessity of incorporating transport limitations in simulation models to optimize the drying process for battery electrode production. However, the simulations were performed for a single-sheet laboratory setup and not a roll-to-roll machine.

Lippke et al. [5] describe a comprehensive numerical simulation framework for the drying process in lithium-ion battery anode production, focusing on the incorporation of non-spherical, flake-like graphite particles. Utilizing the Discrete Element Method (DEM), the drying model integrates drying kinetics, binder migration, and microstructure formation to accurately predict layer thickness and porosity. The model accounts for the complex geometry of graphite particles, enhancing the realism of the simulation. Validation against experimental data confirms the model's effectiveness in capturing the drying behavior and electrode microstructure. The findings demonstrate that considering non-spherical particle shapes significantly improves the prediction accuracy of drying outcomes, advancing the development of more precise digital twins for battery electrode manufacturing.

Oppegård and colleagues [6] developed a dynamic mathematical model to simulate the electrode drying process. The model incorporates different drying technologies, including convective and infrared drying, to analyse energy requirements and optimize the drying process. Using finite difference methods, the researchers solved the one-dimensional diffusion equations governing mass and heat transfer during drying. Sensitivity analysis identified hot air temperature, initial film thickness, and solvent concentration as the most influential parameters affecting energy consumption and drying rates. The simulation results demonstrated that infrared drying achieves faster drying times compared to convective drying, although it requires more energy for solvent evaporation. The results are, however, not validated with an experimental setup. Overall, the model provides valuable insights for energy optimization and process control in the rapidly growing lithium-ion battery industry.

The study of Huang et al. [7] identified three distinct drying stages: heating, constant rate, and falling rate. In the heating stage, the primary driving force is the increase in electrode temperature. The constant rate stage is dominated by heat transfer between the electrode and the air stream, leading to sustained solvent evaporation. During the falling rate stage, mass transfer within the porous electrode becomes the limiting factor affecting the drying process. The model was validated with experimental data from other publication. The experiments, however, were performed with an abstract laboratory setup. Additionally, the effects of process parameters such as jet temperature and air velocity on drying time and energy consumption were analysed. Based on the insights gained, a three-stage drying process was proposed to reduce energy consumption while maintaining drying efficiency and electrode performance.

Xin Ye et al.[8] conducted an extensive numerical simulation to optimize the drying processes of porous medium electrodes in lithium-ion battery manufacturing, aiming to reduce drying time and energy consumption while enhancing electrode performance. They developed a coupled heat and mass transfer model for convective drying and employed a particle swarm optimization algorithm to determine optimal drying parameters, including temperature and Reynolds number. The numerical model was validated through comparison with experimental results from existing literature, demonstrating its accuracy and reliability. Furthermore, the study introduced a multi-stage drying protocol that effectively prevents binder migration, ensuring a uniform distribution of components within the porous structure.

Various approaches have been developed to model the drying process of lithium-ion battery electrodes, each focusing on specific sections of the electrode and machinery. These models address factors such as thickness, particle shape, and drying technologies while incorporating transport resistances and optimizing energy consumption and drying performance. Key insights include the identification of distinct drying stages and the importance of parameters like temperature and airflow in enhancing drying efficiency. Overall, these studies highlight the necessity of considering electrode structure and machine operation to improve the drying process in battery production.

# 04. Process Simulation Approach

We propose the following approach to a process simulation project, which was followed for the work done in this publication and is shown in Figure 5.

**In step 1**, the model is constructed. In this step, all relevant physical processes are determined as well as the possible simplifications necessary to perform the modelling and parametrization step. In this step the software used for process modelling is also chosen, according to the software's capabilities. Here, only a simplified model is constructed, which contains the necessary physical processes but is usually kept small in geometric properties to minimize computing resources.

**In step 2**, the parametrization is performed. Here, experiments are designed in a controlled environment which either allow the direct parametrization of a model or the implicit parametrization through modelling the experiment. For the latter approach, the experiment is re-created and parameters are chosen to fit the model to the experiment.

Lastly, **in step 3** the model is scaled up and validated through experiments on a relevant scale. The model outcome and experimental quality inspection are compared to determine the accuracy of the model.

| Step 1: Model Design | Step 2: Parametrization | Step 3: Validation |
|---|---|---|
| • Determine relevant physical processes<br>• Identify relevant constraints and simplifications | 2.1 Experimental parametrization<br>• Design and perform set of experiments in controlled environment<br>2.2 Model parametrization<br>• Perform independent parametrization measurements<br>• Couple controlled parametrization experiments to a parametrization model | 3.1 Validation experiment<br>• Perform modeled process on relevant scale.<br>• Determine quality inspection parameters for validation<br>3.2 Validation model<br>• Build scaled-up model with previously determined physics parameters.<br>• Compare model output and quality inspection findings |

Figure 5: Overview off the project approach for process modelling

# 05. Electrode Drying Process Modelling Step 1: Model Design

Some of the above presented modelling approaches for electrode drying focus on the microstructure of the battery slurry. To be industrially relevant, Capgemini Engineering's aim is to consider the entire production equipment as well as the fluid film. If both were to be considered without simplifications, the model would have to move from length scales in meters, i.e., the scale of the equipment, to the scale around 0.1 mm, i.e., the scale of the battery slurry film thickness. This discrepancy makes combining both approaches computationally cumbersome. Thus, we decided to simplify the battery slurry and design it as a homogeneous liquid phase described by an interface, which itself contains information on the fluid film thickness. The surrounding convection drying is described by convective heat and mass transfer inside the model under laminar flow (Re<15000) [9] conditions. The drying process modelling was performed using the software StarCCM+ by Siemens. Two models built in the course of this project were a model re-creating the parametrization experiment, to allow fitting the drying parameters to the experiment, and a model for the validation experiment as a comparison to the actual roll-to-roll process. The following describes the simulated physics in more detail:

Governing equations for each phase and chosen solution method:

### 1. Volume Fraction (VOF): Eulerian approach [12] to solve the laminar air flow of dry air:

The incoming air flow, which is a multiphase gas mixture made up of very low water vapor molecules and largely air, is governed by the continuity (1), momentum (2) and energy equations (3). Hence, a classical finite volume method for solving the Navier stokes equations in fluid mechanics [11,14] and volume fraction approach [10] for multiphase mixture is chosen to be solved. The SIMPLE algorithm is used to couple the pressure-velocity fields (taken from the StarCCM+ library). The multiphase gas mixture at the inlet, outlet and in the drying chamber are solved in each CFD unit cell using equation (4), which is the mass conservation equation in a VOF.

The general 2D steady state equations for convective flow and evaporation [11,14] are given below from equations (1) to (4). In the simulation, complex 3D transient convective flow and evaporation equations were solved.

$$\frac{\partial(\rho u)}{\partial x} + \frac{\partial(\rho v)}{\partial y} = 0 \qquad (1)$$

$$\rho u\frac{\partial(u)}{\partial x} + \rho v\frac{\partial(u)}{\partial y} = -\frac{\partial(p)}{\partial x} + \frac{\partial\left(\mu\frac{\partial u}{\partial x}\right)}{\partial x} + \frac{\partial\left(\mu\frac{\partial u}{\partial y}\right)}{\partial y} \qquad (2)$$

$$\rho u\frac{\partial(v)}{\partial x} + \rho v\frac{\partial(v)}{\partial y} = -\frac{\partial(p)}{\partial y} + \frac{\partial\left(\mu\frac{\partial v}{\partial x}\right)}{\partial x} + \frac{\partial\left(\mu\frac{\partial v}{\partial y}\right)}{\partial y} + \rho g \qquad (2)$$

$$\rho C_P u\frac{\partial(T)}{\partial x} + \rho C_P v\frac{\partial(T)}{\partial y} = \frac{\partial\left(k\frac{\partial T}{\partial x}\right)}{\partial x} + \frac{\partial\left(k\frac{\partial T}{\partial y}\right)}{\partial y} + \dot{Q}\ (Nu) \qquad (3)$$

$$\frac{\partial \int_V \alpha_i\rho_i dV}{\partial t} + \oint_A \alpha_i\rho_i v_i . da = \int_V \sum_{j\neq i}(m_{ij\_}m_{ji})dV \qquad (4)$$

### 2. Fluid Film Physics approach for liquid film drying at the VOF-Film Interface:

A fluid film eulerian approach [13] is used to model the physics of the thin slurry film (0.1 mm range). This involves solving for conservation of its mass and momentum in the domain of interest. The fluid film forms an Interface with the dry air defined by the VOF (refer to 5.1). Consequently, convective heat and mass transport mechanisms take place at the interface of the film and the VOF due to the interaction of air with the slurry. This interaction is governed by equations (5) to (7). The parameters such as the vapor concentration gradient $\frac{\partial W}{\partial y}$ ,diffusion coefficient D, and convective heat transfer number $Nu_{total}$[13] play a crucial role in controlling the evaporation rate at various timelines of the evaporation process [14].

The StarCCM+ fluid film model has the following equation for the mass evaporation rate from the liquid to the vapor phase with the thermodynamic equilibrium at the interface as below in equation (7) [source: StarCCM+ library]. It is governed by equation (5) for mass conservation during the phase change (from liquid to vapor). Equations (6a) and (6b) govern the heat transfer due to convection and diffusion, respectively. [13]

Based on equations 6(b) and (5), one can comprehend the coupled behavior of heat and mass transfer which drives the evaporation rate.

$$\rho u\frac{\partial(W)}{\partial x} + \rho v\frac{\partial(W)}{\partial y} = \frac{\partial\left(\rho D\frac{\partial W}{\partial x}\right)}{\partial x} + \frac{\partial\left(\rho D\frac{\partial W}{\partial y}\right)}{\partial y} \qquad (5)$$

$$Nu_{total} = \frac{hd_h}{k} = Nu_s + Nu_l \qquad (6)$$

$$Nu_s = \frac{-2H}{(Tw - Tm)}\frac{\partial T}{\partial y}, (6a)$$

$$Nu_l = \frac{-2H}{(1 - Ww)}\frac{\rho D H_i^{vap}}{k(Tw - Tm)}\frac{\partial W}{\partial y} \qquad (6b)$$

$$\dot{m}_v = \frac{\dot{Q}_v(Nu_{total}) + \sum_i^{N_v}\Delta h_i^{vap}\rho D\frac{dW}{dy}}{\sum_i^{N_v}\Delta h_i^{vap}W} \qquad (7)$$

### 3. Thermophysical parameters:

| Density $\rho$ (kg/m^3) | Dynamic Viscosity $\mu$ (Pa-s) | Saturation Pressure (Pa) | Thermal Conductivity **k** (W/mK) | Specific heat capacity $C_P$ (J/kgK) | Latent heat of vaporization $\Delta h_i^{vap}$ (kJ/kgK) | Diffusion coefficient D (m^2/s) | Heat of formation (kJ/kgK) |
|---|---|---|---|---|---|---|---|

The above-mentioned parameters are used to control the evaporation rate in the fluid film. The Saturation pressure was governed by the Antoine equation [15], which is dependent on temperature and pressure.

### 4. Boundary and Initial Conditions:

For the drying chamber: Standard experimentally available boundary conditions like inlet velocity and outlet pressure were used to solve the air inlet and outlet, respectively. Temperature and pressure were adjusted to match experimental conditions with low relative humidity (RH) at the inlet and inside chamber. The RH was controlled by its mass fraction.

For the fluid film: The evaporating mass in the fluid film has an outlet boundary condition (BC) for which high-resolution interface capturing was used to define interface between the air and the fluid film surface (refer 5.2).

During the simulation the saturation pressure at the film-VOF interface is governed by the Antoine equation, which is also a very critical parameter in evaporation below the boiling point of a liquid [15].

As a first approach, the porous layer of the electrode is, not actually represented, which we assume to be an appropriate simplification since we also parametrize the drying behavior to emulate the behavior of the actual slurry. Only drying parameters were fitted to the experiment, air-flow in the system was not changed and was adapted from the experimental setup.

# 06. Electrode Drying Process Modelling Step 2: Parametrization

For the parameterization of the simulation model, electrode drying experiments in a highly controlled environment were performed. In the following chapter, the experimental setup is described, and the results of an exemplary experiment are outlined. Subsequently, the parameterization in the simulation tool is explained.

## 6.1 Step 2.1: Experimental parameterization

For the experimental parametrization, a stationary drying test bench was used. Weight (corresponding to the solvent content) and temperature of the electrode are monitored on the test bench during the drying process. The test bench allows the integration and combination of various drying methods, including convection, laser and near infrared drying. For convention drying, the temperature of the incoming air (25°C to 200°C), the air volume flow (up to 1000 l/min) and the dew point of the incoming air can be adjusted. The surface temperature of the material is measured with a thermal imaging camera (±5 K accuracy) and the drying behaviour is measured with a precision scale (max capacity 1000 g, accuracy 1 mg). The key components of the stationary drying test bench are depicted in Figure 6.

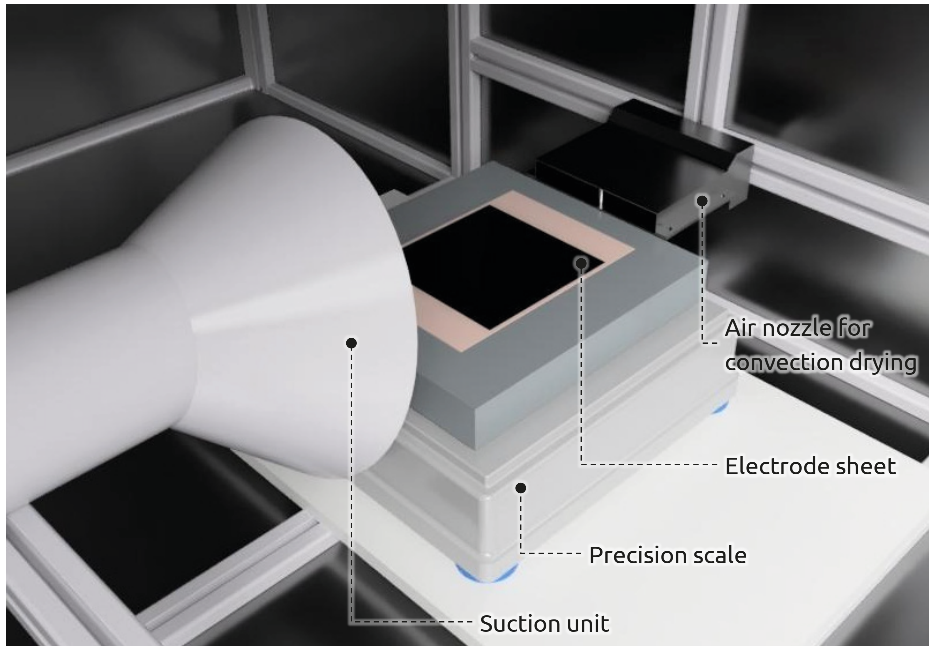

Figure 6: Stationary drying test bench setup

For the experimental parametrization, a series of experiments were conducted on the stationary drying test bench. The experimental workflow encompassed mixing, coating, drying, and post-processing steps. The electrode paste was prepared via twin-screw extrusion mixing. The same electrode paste batch was used for the experimental parameterization and the validation. The electrode (dry) was composed of 95 wt% active material (Graphite), 2 wt% of carboxymethyl cellulose binder, 2 wt% of styrene-butadiene rubber (2nd binder) and 1 wt% of carbon black as conductive additive. Deionized water was used as solvent and the solids content of the electrode paste was 45 wt%.

Immediately before coating, the electrode suspension was stirred again to ensure the uniformity of the material. Subsequently, a defined volume was coated onto copper foil using a doctor blade coating machine (Zehntner ZAA 2600). To realize different area loadings, the wet film thickness of the coatings was varied. A stencil ensured consistent coating areas, resulting in uniform wet weights with low variability. Subsequently, the coated copper foil was transferred to the drying test bench and the drying process was started. During drying, air velocity, temperature (60 °C, 80 °C, and 100 °C), and volume flow were varied to evaluate moisture removal efficiency, while nozzle temperatures were monitored. During post-processing, the measured weight data was smoothed to remove the fluctuation. This systematic approach enabled precise parameterization of the drying model.

One key result of the experiments is the solvent evaporation over time and is shown with the simulation results in Figure 8. In this experiment, an area loading (dry) of 7.75 mg/cm², an air velocity of 2.3 m/s, and an air temperature of 80 °C were used. Initially, a slow drying rate was observed during the heating phase. This was followed by an accelerated drying rate. Subsequently, the drying rate decreased again in the final phase, approaching the completion of solvent evaporation. This behaviour highlights the dynamic changes in drying kinetics under the specified conditions.

Another key result is the surface temperature of the electrode sample. In Figure 7, the surface temperatures at 30s, 180s and 270s are depicted. The electrode paste is heated gradually, starting from the incoming air flow direction. A maximum of 64,5°C was reached with an incoming air temperature of 80°C. The difference between airflow temperature and electrode sample temperature may be caused by a lower temperature on the bottom of the electrode sample.

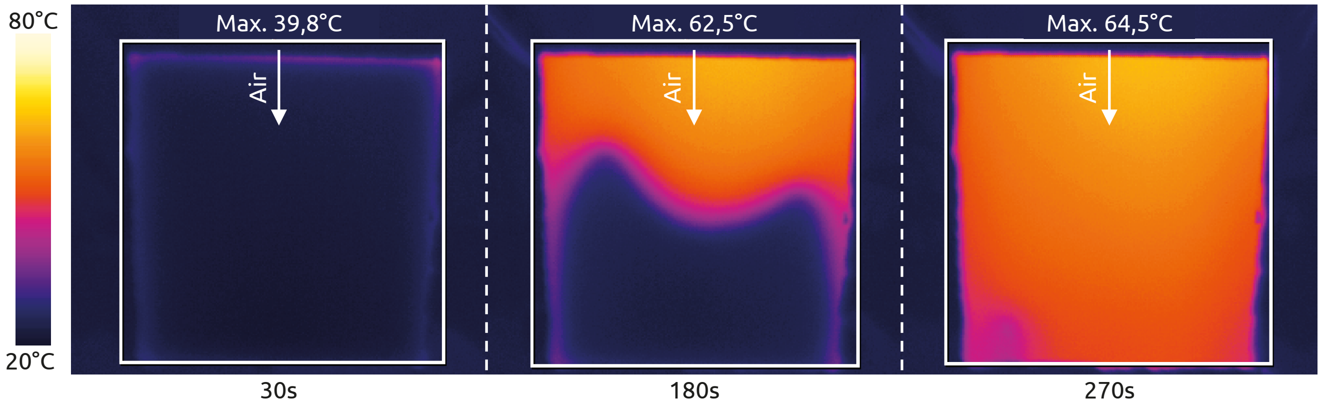

Figure 7: Surface temperature of electrode samples after 30s, 180s, and 270s

## 6.2 Step 2.2: Parametrization model

The experimentally supplied parameters of the parametrization measurements can now be fed into the re-created model experiment. Section 5 described the physics used for the model which now have to be constructed into the proper geometry. Figure 8 shows an x-y axis cut of the parametrization model, which re-creates the experimental environment from step 2.1 (see Figure 6). It shows the temperature profile during the model experiment, which is an example of the more in-depth analysis that can be performed for such a model compared to the experiment. The model can then be used to tune the physical parameters to fit the experimental curve. The parametrization lies at the heart of such a model and is highly time consuming. Ideally it would require an iteration loop back to the model design, as it is the first step to validating the assumptions made during the model design phase. For this work, the model was only tuned to one experiment, however future work would entail the tuning of the specific influence of temperature, layer thickness and convective air speed to account for the effects of evaporation, convective drying and layer diffusion for the model.

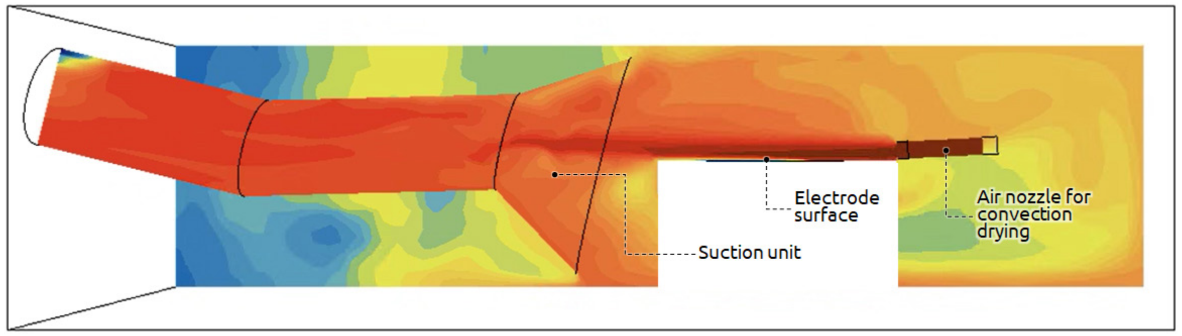

Figure 8: Parametrization model. The model shows a x-y axis cut of the parametrization model of the experimental setup shown in Figure 6.

Figure 9 shows the simulated mass loss (green, blue), experimental mass loss (black) of one of the experiments and the deviation between model and experiments. The unparametrized curve (blue) shows the behavior as if the film was pure water, thus not accounting for effects specific to the slurry. This curve shows larger deviations up to 20% of the experimentally obtained curve. The parametrized curve (green) shows a discrepancy of not more than 10% of the majority of the experimental curve. The remaining deviation can be traced back to simplifications made in the model physics, but are overall in good agreement. For more details on drying mechanisms and model results please contact Capgemini.

## Simulation Curves and Relative Deviations with Experiment Data

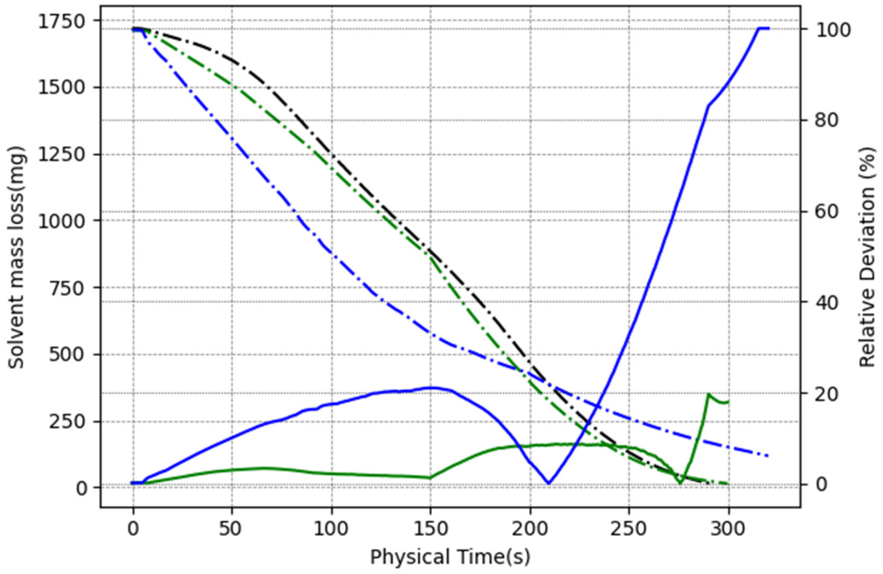

Figure 9: Experimental and model evaluation of the mass loss over time and the . See section 6.1 for the experimental description and setup and section 5 for the model details.

# 07. Electrode Drying Process Modelling Step 3: Validation

## 7.1 Step 3.1: Validation Experiment

The validation of a process model should be performed on a larger scale to ensure reliability of the model. It also should include post-process analysis which can be compared to the process model for further validation. In the following we are describing the validation experiments and the post processing methodology.
Figure 10 shows an picture and the schematic overview over the electrode production equipment.

The electrodes are produced using a roll-to-roll process on a coating system with slot-die coating followed by hot-air convection drying. The slot-die is supplied by a continuously operating progressive cavity pump, which draws from a degassed batch. The coating is applied with a width of 200 mm, centred on a 250 mm wide and 11 µm thick copper foil, at web speeds ranging from 1 to 3 m/min. The target thickness of the dry coating is 75 µm (mass loading of 7 mg/cm2). To continuously monitor the properties of the wet film, it is measured using a confocal line sensor. This ensures that the wet film thickness, edge elevation, width, and position are consistently maintained, which is crucial for the comparability of the various drying processes. The drying process is conducted using close-impact air nozzles inside a flotation oven, where the foil is supported and guided by the airflow. The system features two paired drying chambers, each equipped with five upper and four lower air nozzles. It has an effective drying length of 3 meters and a total effective electrical output of 160 kW. Table 1 sums up the specifications for the equipment.

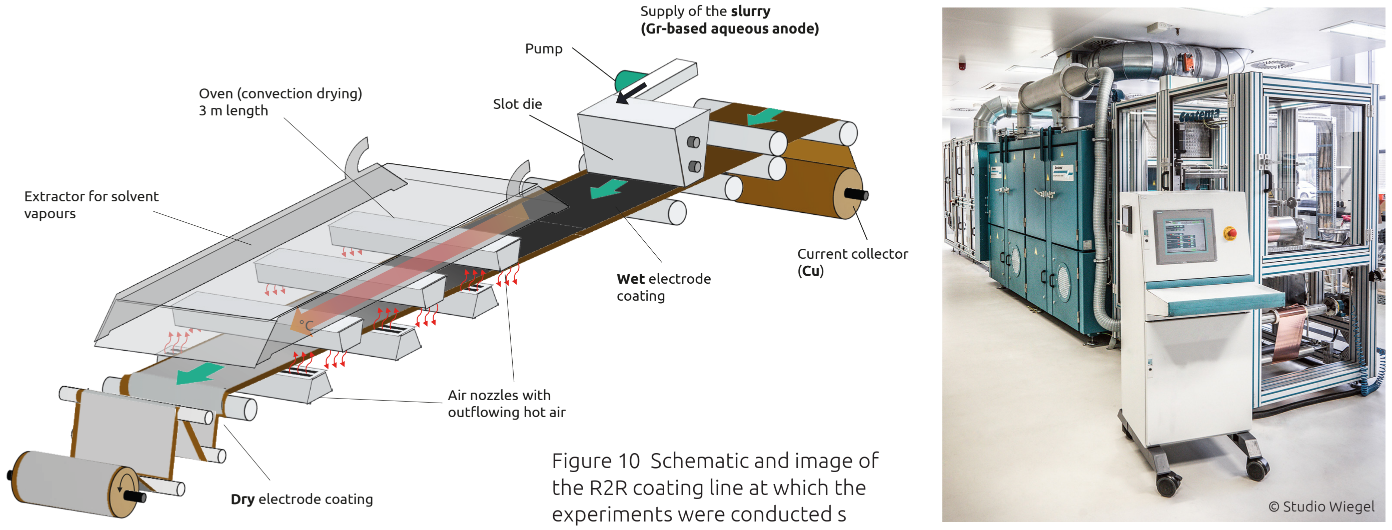

Figure 10 Schematic and image of the R2R coating line at which the experiments were conducted s

| | | |
|---|---|---|
| Coating width | 200 mm | Constant |
| Web width | 250 mm | Constant |
| Coating speed $v_{web}$ | 1 - 3 m/min | Variable |
| Thickness of the wet coating | 155µm | Constant |
| Thickness of the dry coating | 75 µm | Constant |
| Temperature of the oven $T$ | 80 °C | Constant |
| Nozzle volume flow of the oven | 600 - 3500 m³/h | Variable |

Table 1: Equipment specifications of the electrode dryer

## Experimental analysis

### Residual moisture

A thermogravimetric measuring method is used to determine the residual moisture of the electrodes. Therefore, a sample is manually punched out of the R2R process directly after leaving the oven. for this purpose, with which the percentage residual moisture can be calculated from the absolute residual moisture in relation to the total weight of the wet coating.

By definition, the absolute residual moisture $(x_M)$ is the difference between the total sample mass in the wet and dry state and thus describes the change in mass during the measurement. The residual moisture is calculated based on the formula:

$$x_M = \frac{m_{H_2O}}{m_{oo}} = \frac{m_{wet} - m_{dry}}{m_{wet} - m_{cc}} \quad (8)$$

With: $m_{H_2O}$ the mass of the moisture, $m_{oo}$ the overall mass of the electrode (Coating and current collector, $m_{wet}$ the mass of the electrodes after the oven with residual moisture and $m_{dry}$ for the mass of the completely dry electrode (after the measurement and thus after evaporation of the residual moisture).

### Mechanical properties

The mechanical properties of an electrode are crucial for further processing and for the final cell performance. To evaluate the electrodes in this regard, mechanical characterizations such as adhesive pull measurements are carried out.

For inhomogeneous material pairings that have a defined boundary layer, as is the case with the coated anode, the adhesion between the materials can be assumed as a characteristic quality parameter. This can be further subdivided into the adhesion at the material interface, the so-called adhesion, and the adhesion in the separate structures, the cohesion. Regardless of the position, a detachment of the coating must be considered a critical failure for the mechanical integrity of the cell. A measurement of both adhesion values is carried out as part of the evaluation by means of a tensile adhesion test in the direction of the normal vector. In this test, the coated electrode is glued to the film base as well as to the coating surface on opposing sample carriers. The sample carriers are then pressed against each other with a defined force over a constant period of time. The test is then carried out by uniaxially pulling the sample sleds apart until the material bond fails and a continuous force is applied. The maximum tensile force at the onset of material failure represents the mechanical stability of the sample. The obtained value for the maximal force $F_{max}$ then needs to be normalized to the sample area $A$ in order to receive the tensile strength σ of the sample.

$$\sigma = \frac{F_{max}}{A} \quad (9)$$

The following Table 2 shows an excerpt of the results for experimental validation.

| Coating speed [m/min] $v_{web}$ | Nozzle volume flow $Q$ [m$^3$/h] | Residual moisture $x_M$ [%] | Tensile stregth $\sigma$ [N/cm$^2$] | Evaluation |
|---|---|---|---|---|
| 1 | 990 | 2,1 | 90,4 | significantly too dry |
| 1 | 810 | 3,2 | 90,8 | sufficient quality |
| 1 | 690 | 8,2 | 88,4 | significantly too wet |

Table 2: Excerpt of the experiments performed for validation

## 7.2 Step 3.2: Validation Model

The dryer shown above was modelled using the experimentally set input parameters as well as the geometric information of the dryer. Figure 11 shows an image of the physical and model electrode dryer. The model entails the nozzles and upper inlet as well as the outlet of the dryer at the top left in Figure 11 b). For simplification of the model, the nozzles are directly chosen as outlet source to reduce the computational need. For an analysis of the equipment, the air inlet can also be synched with the physical air inlet to simulate the air flow and separation into the nozzles directly.

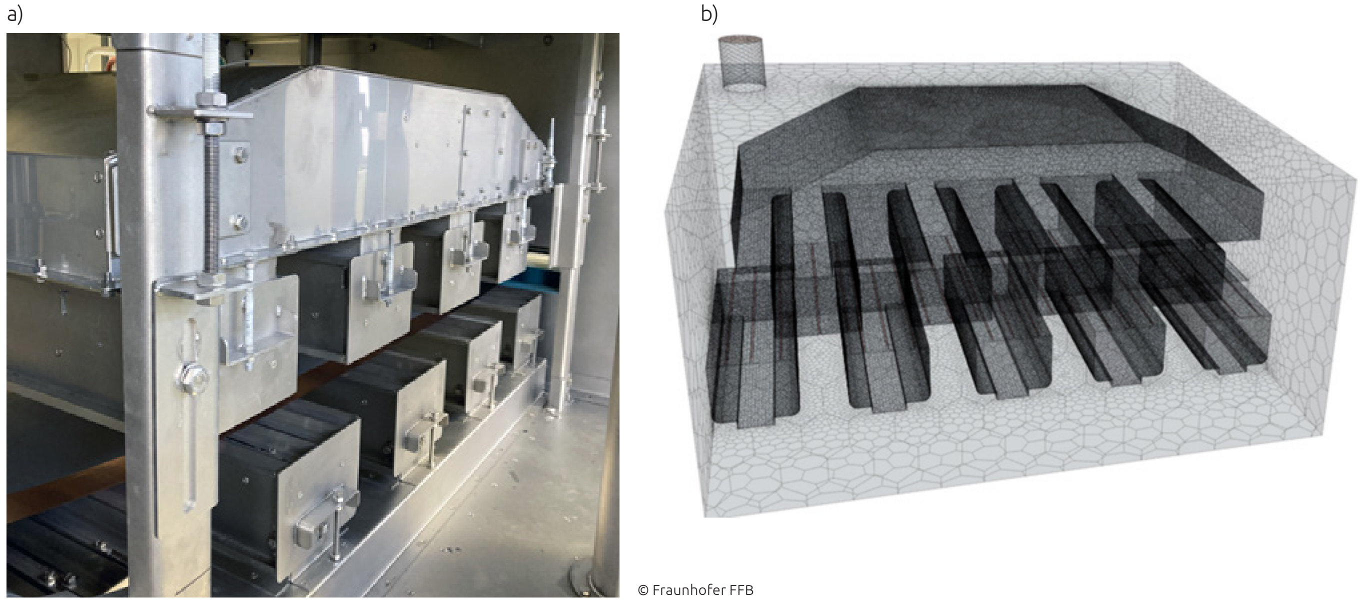

a)

b)

© Fraunhofer FFB

Figure 11: a) Image of the nozzles and electrode line of the electrode dryer;
b) Image of the electrode dryer model with nozzles and electrode layer.

The electrode is represented the same as in the parametrization model, as just a surface without spatial resolution of the slurry. The model can now run the drying simulation. Figure 12 shows an x-y cut of the model after some calculation time expired. This is an example for how these models can be analyzed, by giving temperature distribution profiles throughout the equipment. Similarly, the drying rate across the electrode can be analyzed and be split into specific physical processes such as direct evaporation off the surface or convection, i.e., mass transport from water being adsorbed into the dry air and carried away to the outlets.

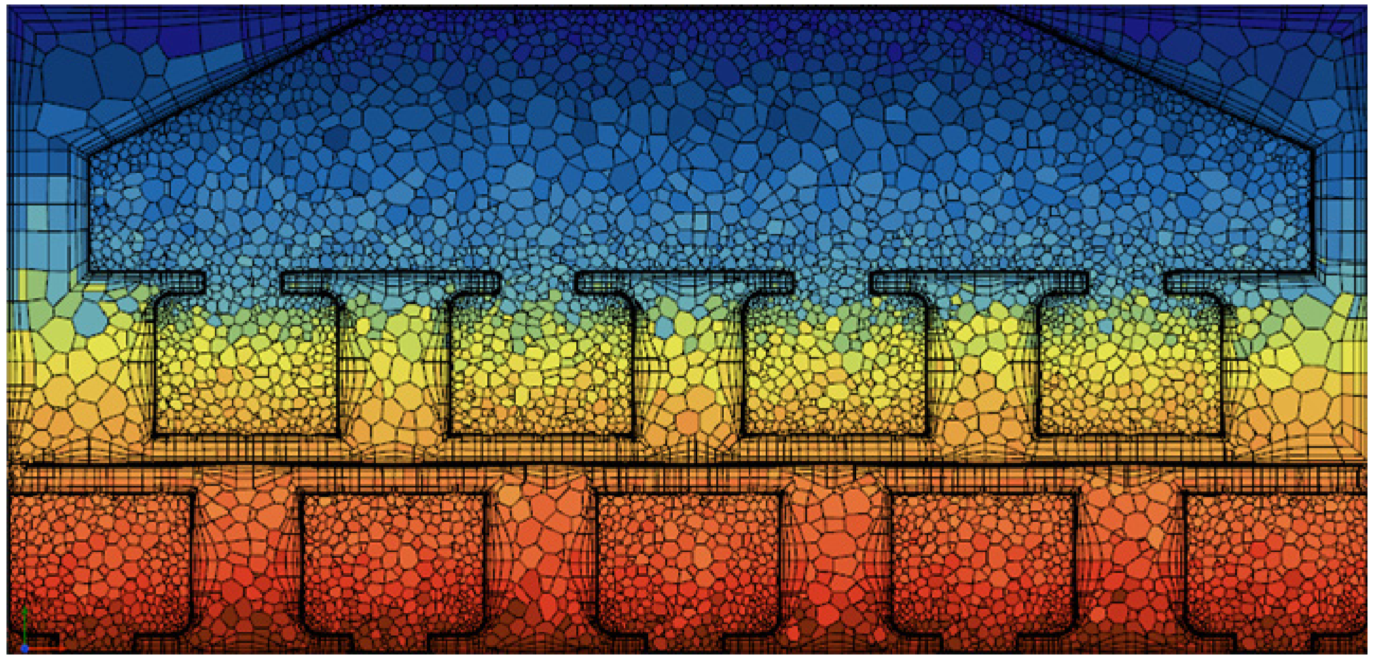

Figure 12: x-y cut of the model center and temperature distribution heat map with meshing overlay.

There are virtually no limits to the analysis possibilities in the model, within the chosen physical boundaries. As mentioned before, the model is flexible in where inlet and outlet boundaries are set. In this instance, the model could also be simplified to include only the nozzles or only half the nozzles. Such a model might still yield qualitatively good results with significantly decreased computational effort. For more information on the model approaches, please contact Capgemini.

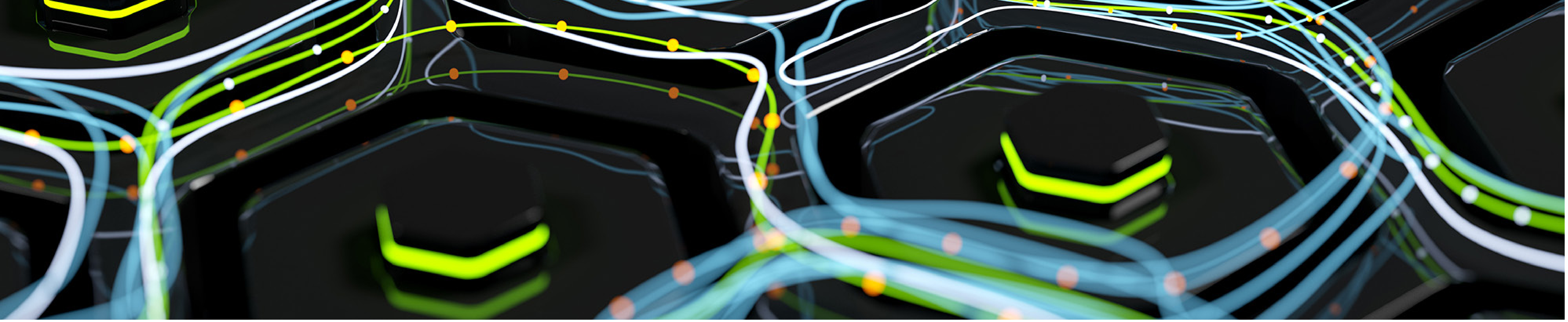

# 08. Analysis of benefits

We estimate that full implementation of process modelling can yield a long term scrap reduction of 1-3%, which for a 50 GWh production facility results in cost savings of 46 – 138 m€ per year (at 92 €/kWh production cost). Additionally, assuming multiple production lines with the same equipment, the work of process modelling is transferable to every piece of equipment and useful to train and support process engineers across multiple production sites. Thus it is scalable and cost efficient. For long term large scale production, the cost to benefit aspect truly can make process simulation highly profitable and thus be a game changer for long term process improvement.

Furthermore, process simulation can be a long term sustainable benefit by raising the level of understanding of the individual processes. For example, a simulation model for electrode drying, as demonstrated in this publication, provides invaluable advantages in understanding the drying process of a specific material and optimizing it for the respective production equipment. During the industrialization from lab scale over pilot scale to giga scale cell production, equipment in different scale is involved in manufacturing the battery cells. Challenges such as maintaining high product quality, reducing scrap rates, and addressing talent shortages become increasingly prominent. Simulation models recreate the physical phenomena of solvent evaporation and heat transfer occurring during electrode drying, offering insights into the complex interplay between production equipment and product that are difficult to observe directly.

**By incorporating the entire drying process – including machinery and relevant surroundings – these models allow process engineers to link simulation parameters directly to machinery inputs.**

This direct linkage facilitates the adjustment and fine-tuning of process parameters, supporting manufacturers in achieving the exacting quality standards required for lithium-ion battery cells. For instance, simulation can predict and mitigate issues like carbon-binder migration caused by rapid drying in high-loading electrodes, or variations in slurry output viscosity after mixing.

Establishing a simulation model for the electrode drying process does require an initial investment in modelling the production equipment; however, this effort is undertaken only once. Additionally, the need for further experimental parameterization is minimal, especially when integrated seamlessly into the existing development-scale electrode development workflows where electrode sheets are already being fabricated. Most notably, the use of simulation significantly reduces the reliance on trial-and-error approaches during process development, potentially cutting the development time by up to 50% through reducing trial and error adjustments especially during new material testing. This acceleration not only streamlines the optimization process but also leads to a substantial reduction in scrap rates, as more accurate and efficient process adjustments minimize material waste.
By accelerating the transition from pilot to giga scale production and decreasing scrap, manufacturers can enhance -overall efficiency and ensure the timely delivery of high-quality lithium-ion battery cells.

# 09. Summary and Outlook

Process simulation can be a highly useful tool to understand the underlying processes of several steps during Li-ion battery cell production, which we have demonstrated here. We have designed the project to aid process engineers.

First, we gave an introduction into process modelling, which intends to be an industrially relevant way of understanding and optimizing production processes and is applied during production steps where relevant physical processes are present. We have described possible model variations for the first four production steps, mixing, coating, drying and calendaring and their benefits, such as improved equipment understanding or processing know-how. The concept of process modelling is embedded in an approach for an end-to-end toolchain, with the ultimate goal to link process and product models.

As part of a more in-depth review, we have demonstrated how electrode drying can be modelled, by performing modelling as well as parametrization and validation experiments.

The model describes the air flow and solvent uptake in the surrounding air, as well as the liquid/gas interface for convective electrode drying, with the electrode represented as an electrode interface and underlying information on solvent content. For parametrization, electrodes were dried in a custom made, stationary setup under various conditions. The setup was then modelled to allow parameter adjustments, improving model accuracy. For validation, a roll-to-roll drying experiment was performed and subsequently modelled. The experimental post-process analysis of the validation experiment allows a more accurate analysis of the model itself.

**Process simulation is a strategic tool, which allows us to take a deeper look in what are sometimes black box processes.**

It requires an understanding of the underlying physics, machine and product properties and modelling know-how, making it highly interdisciplinary. This is why Capgemini has partnered with Production Engineering of E-Mobility Components (PEM) at RWTH Aachen and Fraunhofer Research Institution for Battery Cell Production (FFB) to combine modelling, parametrization and validation experiments to offer an all-in-one service for process modelling.

The Benefits are undoubtedly gaining a fundamental understanding of the interplay between equipment and the intermediary product. With integration of the end-to-end toolchain in product and process development, industrialization efforts for equipment planning and optimization to scale-up future gigafactories can be reduced significantly.

# 10. References

[1] https://www.reuters.com/sustainability/struggling-northvolt-stokes-fear-europes-battery-future-2024-09-13/

[2] von Horstig, Max-Wolfram, et al. “A Perspective on Innovative Drying Methods for Energy-Efficient Solvent-Based Production of Lithium-Ion Battery Electrodes.” Energy Technology 10.12 (2022): 2200689.

[3] Zhang, Ye Shui, et al. “A review of lithium-ion battery electrode drying: mechanisms and metrology.” Advanced Energy Materials 12.2 (2022): 2102233.

[4] Kumberg, Jana, et al. “Reduced drying time of anodes for lithium-ion batteries through simultaneous multilayer coating.” Energy Technology 9.10 (2021): 2100367.

[5] Lippke, Mark, et al. “Coupled numerical simulation of the drying and calendering for Lithium-ion battery anodes with non-spherical particles.” Powder Technology 452 (2025): 120566.

[6] Oppegård, Emil, et al. “Study of an industrial electrode dryer of a lithium-ion battery manufacturing plant: Dynamic modelling.” (2020).

[7] Huang, Tianlun, et al. “Modeling and analysis of solvent removal during lithium-ion battery electrode drying: A semi-conjugate approach.” Chemical Engineering Science 301 (2025): 120777.

[8] Ye, Xin, et al. “Optimizing porous medium electrode suspension drying: A numerical simulation.” Physics of Fluids 36.7 (2024).

[9] Ting, David. Basics of engineering turbulence. Academic Press, 2016.

[10] Yadigaroglu, George, and Geoffrey F. Hewitt, eds. Introduction to multiphase flow: basic concepts, applications and modelling. Springer, 2017.

[11] Lin, T. F., et al., Analysis of Combined Buoyancy Effects of Thermal and Mass Diffusion on Laminar

Forced Convection Heat Transfer in a Vertical Tube, ASME J. Heat Transfer, 110 (1988), 2, pp. 337-344

[12] Jones, Bevan W. S. et al. “The initialisation of volume fractions for unstructured grids using implicit surface definitions.” Computers & Fluids (2019)

[13] Mir, R. (2015). Numerical study of heat and mass transfer during evaporation of a thin liquid film. Thermal Science, 19(5), 1805-1819

[14] Ilona Machovská, Tomáš Hyhlík, CTU in Prague, Faculty of mechanical engineering, Department of fluid dynamics and thermodynamics, Technická 4, 166 07 Prague 6, Czech republic

[15] Yaws, Carl L. The Yaws handbook of vapor pressure: Antoine coefficients. Gulf Professional Publishing, 2015.

# 11. Acknowledgement

We would like to thank **Siemens** for providing the license and for support while defining the physics phase of the model.

Furthermore, we would like to express our gratitude to **Simon Straub**, **Felix Böhme**, **Justin Korthaus** and **Matthias Tente** for independently conducting the coating and drying experiments during the parameterization phase.

Additionally, we sincerely thank **Lennart Keil** and **Jan Wittenmeier** for their significant contributions to the evaluation of the experiments.

# 12. About the authors

Capgemini

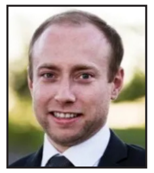

**Michael Müller**

Head of Climate Tech & Sustainability

**Markus Fiege**

Head of Center of Excellence Battery

**Dr. Christoph Weißinger**

Virtual Battery Development Lead

**Jens Radtke**

Battery Development Expert

**Dr. Robert Morasch**

Process Expert

**Shreyas Shetty**

Simulation Expert

PEM | RWTH AACHEN UNIVERSITY

**Prof. Dr.-Ing. Achim Kampker**

University Professor & Founder & Managing Director at Fraunhofer FFB

**Prof. Dr.-Ing. Heiner Heimes**

Member of Institute Management

**Henrik Born**

Chief Engineer

**Sebastian Wolf**

Group Lead

**Matthias Smulka**

Research Associate

**Sven Kemmer**

Research Associate

Fraunhofer
FFB

**Dr. Kristina Borzutzki**

Group Manager Process Engineering

## Follow us.

Capgemini

PEM | RWTH AACHEN UNIVERSITY

Fraunhofer
FFB

# About

**Capgemini** is a global business and technology transformation partner, helping organizations to accelerate their dual transition to a digital and sustainable world, while creating tangible impact for enterprises and society. It is a responsible and diverse group of 340,000 team members in more than 50 countries. With its strong over 55-year heritage, Capgemini is trusted by its clients to unlock the value of technology to address the entire breadth of their business needs. It delivers end-to-end services and solutions leveraging strengths from strategy and design to engineering, all fueled by its market leading capabilities in AI, generative AI, cloud and data, combined with its deep industry expertise and partner ecosystem. The Group reported 2024 global revenues of €22.1 billion.

**www.capgemini.com**

The **Chair of Production Engineering of E-Mobility Components (PEM) of RWTH Aachen** University was founded in 2014 by Professor Achim Kampker and has been active in the field of lithium-ion battery production technology for many years. PEM covers all aspects of the development, production, and re-cycling of battery cells and systems. Due to numerous industrial projects with companies of all stages of the value chain and central positions in renowned research projects, PEM offers extensive expertise.

**www.pem.rwth-aachen.de**

The **Fraunhofer Research Institution for Battery Cell Production FFB** is a facility of the Fraunhofer-Gesellschaft at the Münster site. Its concept provides for a combination of laboratory and production research for different battery cell formats - round cell, prismatic cell and pouch cell. Fraunhofer FFB employees research individual process steps or the entire production chain as required. Together with the project partners – Münster Electrochemical Energy Technology (MEET) at the University of Münster, the Chair PEM of the RWTH Aachen and the Research Center Jülich – the Fraunhofer-Gesellschaft is creating an infrastructure in Münster that will enable small, medium-sized and large companies, as well as research institutions, to test, implement and optimize the near-series production of new batteries. As part of the “FoFeBat” project, the German **Federal Ministry of Education and Research** and the **state of North Rhine-Westphalia** are funding the establishment of the Fraunhofer FFB with a total of approximately **820 million EUR**. The federal government is providing up to 500 million EUR for research facilities and projects at the Fraunhofer FFB, while the state of North Rhine-Westphalia is investing around 320 million EUR in land and new buildings.

**www.fraunhofer.de**

Get the future you want